Syntheses and third-order NLO properties of η^6 complexes of *N*-ethylcarbazole with $Cr(CO)_3$ and $Cr(CO)_2PPh_3$ moieties†

Yanchao Che, Xiaohui Tian,* Hui Chen, Zhenyu Tang and Jiaping Lin

Received (in Montpellier, France) 4th January 2006, Accepted 4th April 2006
First published as an Advance Article on the web 27th April 2006
DOI: 10.1039/b518346d

Carbazole mono- and bimetallic complexes [(*N*-ethylcarbazole){$Cr(CO)_3$}$_2$] (**3**) and [(*N*-ethylcarbazole)$Cr(CO)_2$L] (L = CO (**2**) and PPh_3 (**4**)) have been synthesized, and X-ray crystal structure analyses performed for **2** and **4**. Each complex possesses spectroscopically intense intraligand (IL) and metal-to-ligand charge-transfer (MLCT) excitations that are well separated in energy. The MLCT bands display a small to moderate negative solvatochromism. The third-order non-linear optical (NLO) properties, measured by the time-resolved forward degenerate four-wave mixing (DFWM) technique in solution at 532 nm, have been studied for these complexes, together with *N*-ethylcarbazole for comparison. It is found that the third-order NLO response can be tuned by chromium complexation. The molecular second-order hyperpolarizabilities, γ, of the synthesized complexes are determined to be in the order of 10^{-30} esu and clearly depend on both the nature of the ligand and the extent of chromium tricarbonyl coordination by the carbazole ring. The carbazole-mediated metal–metal electronic interaction existing in **3** is believed to be a possible factor responsible for a large improvement in the non-linearity.

Introduction

There has been considerable interest in the non-linear optics (NLO) of organometallic compounds that possess low-energy metal-to-ligand charge-transfer (MLCT) or ligand-to-metal charge-transfer (LMCT) excitations,[1] because these effects can exert additional control on the optoelectronic properties through the oxidation state of the metal and the nature of the attached ligands. Moreover, the interaction of d-orbitals of the transition metal with π-orbitals of the organic moiety offers new ways of enhancing the non-linear response. To date, several useful reviews of the NLO behavior of organometallic compounds have been published.[2] Among the enormous variety of metallic sub-units that can be attached to π-conjugated organics, the $Cr(CO)_3$ moiety has been a target of focus due to its high polarity, the amphoteric nature of its electrons and its rich chemistry.[3] Enhancement of the first-order hyperpolarizability, β, of alkynylated and alkenylated arenes upon $Cr(CO)_3$ complexation has been theoretically predicted and experimentally corroborated.[2d,4] Cheng *et al.* measured the second-order hyperpolarizability, γ, of $Cr(CO)_3$–benzene (CBC) complexes and found that small changes in the substituents attached to the benzene ring could produce a major effect on the non-linear response.[5] This implies that correctly designed molecules of this type may act as useful NLO materials. On the other hand, the carbazole unit is known as a hole-transporting and electroluminescent structure; its simple functionalization allowing the preparation of attractive molecules with multi-functional properties[6] such as photoconductivity,[7] optical non-linearity[8] and photorefractivity.[9] Nisoli *et al.* reported that uniaxially-oriented films of poly[1,6-di(*N*-carbazolyl)-2,4-hexadiyne] exhibit a very large resonant third-order NLO susceptibility, $\chi^{(3)}$, up to 2×10^{-7} esu.[10] Recent results show that enhanced γ values can be readily obtained in carbazole derivatives by extending the conjugation length, altering the substituted positions, or choosing appropriate substituents.[11] With the above considerations in mind, we have designed a series of metallocarbazole chromophores with novel bonding patterns and coordination geometries which permit spatial arrangements of atoms that may not be easily accessible in other systems, resulting in an increase in design flexibility. The $Cr(CO)_3$ group is incorporated into the carbazole ring in order to allow the fine-tuning of its electronic/optical properties, and moreover, the realization of new properties resulting from synergistic effects.[12] By replacing one CO group by another ligand, organometallic chromophores with different absorption bands (linear and non-linear) can be prepared. We describe in this paper the syntheses and structures of [(*N*-ethylcarbazole){$Cr(CO)_3$}$_2$] (**3**) and [(*N*-ethylcarbazole)$Cr(CO)_2$L], where L = CO (**2**) and PPh_3 (**4**) (Scheme 1), as well as the effects of the metal and its ligand on their linear and non-linear optical properties. Considering that the different substituents can be easily introduced into the carbazole ring,[13] it should be noted that these complexes seem to be intriguing candidates as chromophoric segments for the future development of organometallic NLO polymers.

School of Materials Science and Engineering, East China University of Science and Technology, Shanghai 200237, China. E-mail: tianxh@263.net; Fax: +86 21-54288175

† Electronic supplementary information (ESI) available: ^{1}H NMR and IR spectra of **2–4**, and full crystallographic summary data for **2** and **4**. For data in CIF or other electronic format see DOI: 10.1039/b518346d

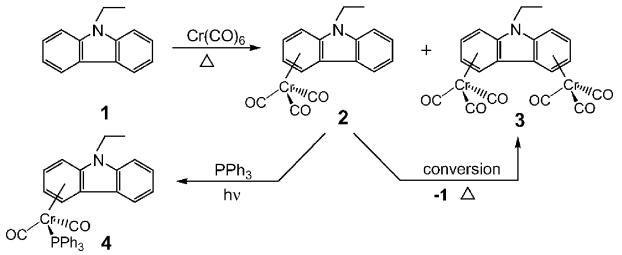

Scheme 1

Experimental

General procedures

Unless otherwise noted, all manipulations with air-sensitive materials were performed under a nitrogen atmosphere using standard Schlenk techniques and a Vacuum Atmospheres dry box. Solvents were freshly distilled over appropriate drying reagents, and all Schlenk flasks were flame-dried under vacuum prior to use. $Cr(CO)_6$ (99%, Strem Chemistry) was sublimed prior to use. *N*-ethylcarbazole (95%, Aldrich) was used as received. Elemental analyses were carried out on Elementar Vario EL III (C, H, N) and TJARIS 1000 (Cr) analyzers, respectively. Electron impact mass spectra were recorded on a Micromass GCT (EI, 70 eV) mass spectrometer. ^{1}H NMR (500 MHz) and ^{13}C NMR (125 MHz) spectra were recorded on a Bruker AVANCE 500 MHz spectrometer using $CDCl_3$ as solvent at 298 K and Me_4Si as an internal standard. IR spectra were recorded on a Nicolet Magna-IR 550 instrument using KBr pellets. Column chromatography was performed on Matrix silica (60–90 μm). UV-vis spectra were obtained on a Varian Cary 500 spectrophotometer rebuilt by OLIS to incorporate computer control. Melting points were measured using a Reichert Thermopan melting point microscope and were uncorrected.

Syntheses of mono- (2) and bis-$Cr(CO)_3$ (3) complexes of *N*-ethylcarbazole

A mixture of *N*-ethylcarbazole (1.46 g, 7.5 mmol) and freshly sublimed $Cr(CO)_6$ (3.30 g, 15.0 mmol) in di-*n*-butylether (85 mL) and dioxane (12 mL) was heated under reflux (bath temperature: 150 °C) for 30 h. After being cooled, the solution was filtered through a Celite filter and the clear solution concentrated until a solid appeared. The residue was extracted into 10 mL of CH_2Cl_2 and passed through a 5 × 35 cm column of silica gel, eluting with CH_2Cl_2/petroleum ether (1 : 3 v/v). Two bands were observed: the first yellow band (complex **2**; MS (*m*/*z*): 331 $[M]^+$) was collected with ~500 mL of the eluent, and the second orange band (complex **3**; MS (*m*/*z*): 467 $[M]^+$) collected with ~300 mL of eluent. The products were recrystallized twice from CH_2Cl_2/*n*-hexane (3 : 1 v/v), respectively, to obtain light yellow crystals of **2** and orange microcrystals of **3**.

Complex **2**: Yield 1.33 g (53.7%). Mp 141–142 °C. Anal. calc. for $C_{17}H_{13}NO_3Cr$: C, 61.63; H, 3.93; N, 4.23; Cr, 15.71; found: C, 61.75; H, 3.87; N, 4.19; Cr, 15.82%. UV-vis (CH_2Cl_2, λ_{max}/nm (10^4 ε/cm^{-1} mol^{-1} dm^3)): 395 (1.1) and 331 (2.1). IR (KBr, ν/cm^{-1}): 1936, 1850, 1554, 1471, 1435 and 1324. ^{1}H NMR (500 MHz, $CDCl_3$) δ: 1.50 (t, 3 H, J = 14.6 Hz), 4.18 (m, 2 H), 5.10 (t, 1 H, J = 12.5 Hz), 5.62 (t, 1 H, J = 12.9 Hz), 5.89 (d, 1 H, J = 6.9 Hz), 6.62 (d, 1 H, J = 6.4 Hz), 7.27 (t, 1 H, J = 17.9 Hz), 7.32 (d, 1H, J = 8.2 Hz), 7.50 (t, 1 H, J = 15.4 Hz) and 7.91 (d, 1 H, J = 7.8 Hz). ^{13}C NMR (125 MHz, $CDCl_3$) δ: 14.22, 38.80, 75.04, 85.83, 89.34, 92.66, 93.41, 110.06, 120.83, 121.55, 123.15, 123.76, 128.27, 142.76 and 234.72. MS-EI (70 eV, *m*/*z* (%)): 331 $[M^+]$ (7.0), 247 $[M^+ - 3CO]$ (100.0), 195 $[M^+ - Cr(CO)_3]$ (12.6) and 52 $[Cr^+]$ (41.8).

Complex **3**: Yield 0.21 g (6.0%). Mp 184–185 °C (dec.). Anal. calc. for $C_{20}H_{13}NO_6Cr_2$: C, 51.39; H, 2.78; N, 3.00; Cr, 22.27; found: C, 51.31; H, 2.89; N, 2.93; Cr, 22.35%. UV-vis (CH_2Cl_2, λ_{max}/nm (10^4 ε/cm^{-1} mol^{-1} dm^3)): 432 (0.7) and 346 (1.6). IR (KBr, ν/cm^{-1}): 1939, 1902, 1853, 1530, 1506, 1452, 1433 and 1347. ^{1}H NMR (500 MHz, $CDCl_3$) δ: 1.55 (t, 3 H, J = 21.3 Hz), 3.98 (m, 2 H), 5.07 (t, 2 H, J = 12.3 Hz), 5.59 (t, 2 H, J = 12.7 Hz), 5.73 (d, 2 H, J = 6.8 Hz) and 6.42 (d, 2 H, J = 6.3 Hz). ^{13}C NMR (125 MHz, $CDCl_3$) δ: 13.91, 30.39, 74.65, 85.86, 87.54, 92.33, 93.50, 125.05 and 233.37. MS-EI (70 eV, *m*/*z* (%)): 467 $[M^+]$ (6.0), 383 $[M^+ - 3CO]$ (4.5), 299 $[M^+ - 6CO]$ (10.7), 195 $[M^+ - 2Cr(CO)_3]$ (2.8) and 52.0 $[Cr^+]$ (27.5).

Synthesis of [(*N*-ethylcarbazole)$Cr(CO)_2PPh_3$] complex (4)

2 (0.5 g, 1.5 mmol) and triphenylphosphine (0.59 g, 2.3 mmol, recrystallized from ethanol) were irradiated in 75 mL of dry benzene, in a Schlenk tube, under a Hanovia ultraviolet lamp, with continuous stirring, under a nitrogen atmosphere, for 8 h. The heat from the lamp allowed the reaction mixture to reflux. The dark violet solution was filtered hot through a glass frit and rinsed with *n*-hexane to obtain 0.30 g (35.2%) of a violet solid which was stable to air. Recrystallization from dry, degassed CH_2Cl_2/*n*-hexane (3 : 1 v/v) yielded large, dark-violet crystals. Mp 160–161 °C (dec.). Anal. calc. for $C_{34}H_{28}NO_2PCr$: C, 72.21; H, 4.96; N, 2.48; Cr, 9.20; found: C, 72.13; H, 4.88; N, 2.51; Cr, 9.25%. UV-vis (CH_2Cl_2, λ_{max}/nm (10^3 ε/cm^{-1} mol^{-1} dm^3)): 422 (3.6) and 351 (6.1). IR (KBr, ν/cm^{-1}): 1856, 1795, 1539, 1470, 1433 and 1329. ^{1}H NMR (500 MHz, C_6D_6) δ: 1.28 (t, 3 H, J = 14.2 Hz), 3.72 (m, 2 H), 4.58 (t, 1 H, J = 11.1 Hz), 4.96 (m, 2 H), 5.42 (t, 1 H, J = 4.4 Hz), 7.08 (d, 1 H, J = 7.9 Hz), 7.17 (d, 1 H, J = 8.2 Hz), 7.22 (s, 9 H) and 7.47 (m, 2 H) and 7.62 (m, 6 H). ^{13}C NMR (125 MHz, $CDCl_3$) δ: 14.43, 39.36, 71.57, 85.06, 89.46, 91.59, 109.24, 119.46, 120.41, 121.05, 126.35, 126.71, 128.34, 129.27, 133.69, 134.55, 139.97, 140.25 and 242.48. MS-EI (70 eV, *m*/*z* (%)): 565 $[M^+]$ (1.3), 509 $[M^+ - 2CO]$ (20.0), 314 $[CrPPh_3^+]$ (43.6), 262 $[PPh_3^+]$ (100.0), 195 $[M^+ - Cr(CO)_2PPh_3]$ (32.1) and 52 $[Cr^+]$ (26.9).

Crystallography

Single crystals of **2** and **4** suitable for X-ray diffraction were obtained by recrystallization from CH_2Cl_2/*n*-hexane at −5 °C under an inert atmosphere, and were sealed in thin-walled glass capillaries. Data were collected on a Bruker Smart Apex CCD diffractometer with graphite-monochromated Mo-Kα radiation (λ = 0.71073 Å) using the ω-2θ technique at 293 K. Both structures were solved by direct methods using SHELXS-97 and refined by the full-matrix least-squares

Table 1 Details of data collection and structure refinement for **2** and **4**

	2	**4**
Empirical formula	$C_{17}H_{13}$ Cr NO_3	$C_{35}H_{30}Cl_2CrNO_2P$
Formula weight	331.28	650.47
Crystal system	Monoclinic	Triclinic
Space group	$P2(1)/c$	P-1
Color, form	Yellow, blocks	Violet, blocks
a/Å	8.7347(7)	10.0091(9)
b/Å	11.5839(9)	10.7369(10)
c/Å	14.6847(11)	14.6282(14)
α/°	90	90.880(2)
β/°	90.8290(10)	90.925(2)
γ/°	90	101.742(2)
V/Å^3	1485.7(2)	1538.7(2)
Z	4	2
$d_{calc.}$/g cm^{-3}	1.481	1.404
Absorption coefficient/mm^{-1}	0.781	0.631
F(000)	680	672
Crystal size/mm	0.489 × 0.325 × 0.237	0.486 × 0.432 × 0.120
θ range/°	2.24 to 27.00	1.39 to 27.00
No. of reflections collected	8541	9054
No. of unique data	3212	6528
No. of data/restraints/parameters	3212/0/217	6528/2/375
R_{int}	0.0701	0.0520
GOF/F^2	1.021	1.112
R indices [$I > 2\sigma(I)$] [a,b]	R_1 = 0.0402 wR_2 = 0.1098	R_1 = 0.0699 wR_2 = 0.2109
R indices (all data)	R_1 = 0.0469 wR_2 = 0.1141	R_1 = 0.0851 wR_2 = 0.2249
Largest differential peak and hole (eÅ^{-3})	0.407/−0.550	1.948/−1.079

[a] $R_1 = \Sigma||F_o| - |F_c||/\Sigma|F_o|$. [b] $wR_2 = \{\Sigma[w(F_o^2 - F_c^2)^2]/\Sigma[w(F_o^2)^2]\}^{\frac{1}{2}}$.

method on all F^2 data using the program SHELXL-97.[14] There was a CH_2Cl_2 solvate in the unit cell of complex **4**. All non-hydrogen atoms were refined anisotropically. Hydrogen atoms were inserted in idealized positions and refined using a riding model. Relevant crystallographic information is summarized in Table 1.

NLO measurement

The third-order NLO properties of the studied compounds were measured using the technique of time-resolved forward degenerate four-wave mixing (DFWM). Fig. 1 shows a schematic diagram of the geometry of the light beams used in the DFWM experiments.

The excitation source was a mode-locked Nd:YAG laser system (wavelength 532 nm, pulse width 35 ps, repetition rate 10 Hz, pulse energy 1.5 mJ). The incident laser beam was split into two pump beams, k_1 and k_2, and a probe beam, k_3, through reflecting beam splitters. They were then temporally and spatially overlapped into the sample with a 205 mm focal length lens. The signal beam, k_4, was collected by a photodiode and then analyzed by a boxcar and computer. In the experiment, the sample dissolved in CH_2Cl_2 was placed in a 1 mm quartz cell and the intensity of the DFWM response for the solution samples, corresponding to the maximum of the temporal profiles obtained by scanning the delay, was compared to the signal obtained for a reference sample (CS_2 was employed in our case; its $\chi^{(3)}$ value was 6.8×10^{-13} esu at 532 nm) under the same light intensity conditions. The $\chi^{(3)}$ value and the non-linear refractive index, n_2, of the samples were then calculated from eqn (1) and eqn (2), respectively.[15]

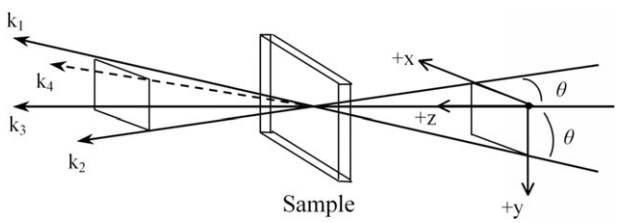

Fig. 1 Schematic diagram of the geometry of the light beams in a four-wave mixing experiment.

$$\chi^{(3)} = \left(\frac{I_4}{I_{4r}}\right)^{1/2} \frac{d_r}{d} \left(\frac{n}{n_r}\right)^2 \frac{\alpha d \exp\left(\frac{\alpha d}{2}\right)}{1 - \exp(-\alpha d)} \chi_r^{(3)} \qquad (1)$$

$$n_2 = \frac{12\pi\chi^{(3)}}{n} \qquad (2)$$

where α is the linear absorption coefficient, I_4 refers to the intensity of the conjugate signal, d is the thickness of the sample, n is the linear refractive index of the medium and the subscript 'r' refers to the reference sample counterpart. For molecular systems, the second-order hyperpolarizability, γ, is related to $\chi^{(3)}$ by eqn (3).[16]

$$\gamma = \frac{\chi^{(3)}}{L^4 N} \qquad (3)$$

Here, L ($L = (n^2 + 2)/3$) is the local field factor approximated by the Lorentz expression, n is the linear refractive index of the solvent and N represents the number density of the compound.

Results and discussion

Syntheses and structural characterization

The reaction of *N*-ethylcarbazole (**1**) with 2 equivalents of $Cr(CO)_6$ in di-*n*-butylether and dioxane (7 : 1 v/v) gives a mixture of **2** and **3** in a 9 : 1 ratio. Attempts to improve the yield of **3** using excess chromium reagent, a high boiling point solvent and prolonged reaction time, failed. Heating pure **2** in dioxane at temperatures up to 110 °C under an inert atmosphere for several hours gives rise to a conversion to **3**, but the reverse process is not feasible for the conversion of **3** into **2** under the same conditions. The sequence of events indicates that mononuclear complex **2** is the kinetic product, which subsequently rearranges to the corresponding binuclear complex **3** and free ligand **1** as the thermodynamically more stable products.[17] EI-mass spectra of **2** and **3** show peaks of highest mass corresponding to their monomeric formulas, respectively. The infrared spectra of **2** and **3** in the carbonyl stretching region are very different: two bands are seen in **2** (ν_{CO} = 1936 and 1850 cm^{-1}), while **3** has three bands (ν_{CO} = 1939, 1902 and 1853 cm^{-1}), reflecting some coupling of the CO vibration of the $Cr(CO)_3$ units in the latter case. In the proton and carbon NMR spectra, the characteristic high-field shift of the complexed arene carbon and proton resonances not only facilitates the unambiguous assignment of the carbazole

signals but also clearly indicates the mutual electronic influence of both coordinated rings for the dichromium species.[18]

Further reaction of **2** with 1.5 equivalents of triphenylphosphine in benzene gives **4** as a violet solid. We tried to replace **2** by **3** in this reaction, but no *N*-ethylcarbazole–bis(Cr$(CO)_2PPh_3$) complex was found as a product; the reactions involved appearing to be non-specific. Complex **4** is stable to air and moisture in the solid state but decomposes slowly in solution at room temperature. The EI mass spectrum of **4** shows the highest mass peak for the molecular ion, $[M]^+$, with a relative intensity of 1.3%. The IR spectrum reveals two CO stretching bands (ν_{CO} = 1856 and 1795 cm^{-1}) that are shifted to lower energies (compared to **2**), suggesting a distinct mutual influence of the individual ligands *via* the metal center. Similar electronic effects are also noted in the carbon and proton resonances of the coordinated ring in the NMR spectra, *i.e.* shifted to high-field, while the carbonyl carbon resonances are slightly shifted to low-field.

The structures of **2** and **4** have been determined by X-ray crystallography.‡‡ The molecular structures and selected bond lengths and angles are shown in Fig. 2 and Table 2, respectively. Attempts to grow X-ray quality crystals of **3** in various solvents at different temperatures have been unsuccessful to date. Complexes **2** and **4** are intrinsically asymmetric molecules and crystallize in the monoclinic and triclinic crystal systems, with space groups $P2(1)/c$ and $P\text{-}1$, respectively. There is a CH_2Cl_2 solvate in the unit cell of complex **4**. To probe the effect of ligand exchange, some useful comparisons between the complexes can be made concerning the coordination geometry around the metal center. Complex **2** exhibits an expected three-legged piano stool structure, having a staggered conformation, with one carbonyl group being disposed above the central heterocycle.[3c] Replacing one CO with a triphenylphosphine ligand, as in **4**, causes a rotation about the Cr–c(0) [c(0) = coordinated ring centroid] axis that forces the Cr–P bond into a position opposite the *N*-ethyl group in response to the steric requirements of the PPh_3 group, one phenyl ring of which is less susceptible to the steric bulk and electronic influences of the coordinated ring than the other two. The phosphine ligand, which enhances the electron density along the Cr–PPh_3 bond axis, strengthens the Cr–CO bonds and weakens the C–O bonds, as shown by the variation in the corresponding bond lengths. The distance of the chromium from the mean plane in **2** is 1.752 Å, which is comparable to that in **4** (1.749 Å), suggesting that the metal–carbazole bonding seems to be less sensitive to the nature of the ligand. The carbazole ring and its attached *N*-methene carbon are nearly coplanar, although slight deviations from planarity are observed in the coordinated aryl ring (planar to within 0.032 Å for **2** and 0.055 Å for **4**). The C–C distances within the coordinated ring are routinely longer than those in the uncoordinated aryl ring (average 1.406/1.388 Å for **2** and 1.408/1.393 Å for **4**). This is likely to reflect a slight loss in aromaticity upon coordination, owing to back-donation of electron density from the metal into the π* orbitals of the ring. A similar situation has been found for several (stilbene)Cr$(CO)_3$ compounds, in which the electron density is localized on the coordinated ring rather than spread out over the entire molecular configuration.[3a] In complexes **2** and **4**, the differences between the two aryl rings of the carbazole can lead to an increase in the magnitude of the permanent dipolar moment along the carbazole plane.

‡ CCDC 291883 (**2**) and CCDC 291884 (**4**). For crystallographic data in CIF or other electronic format see DOI: 10.1039/b518346d

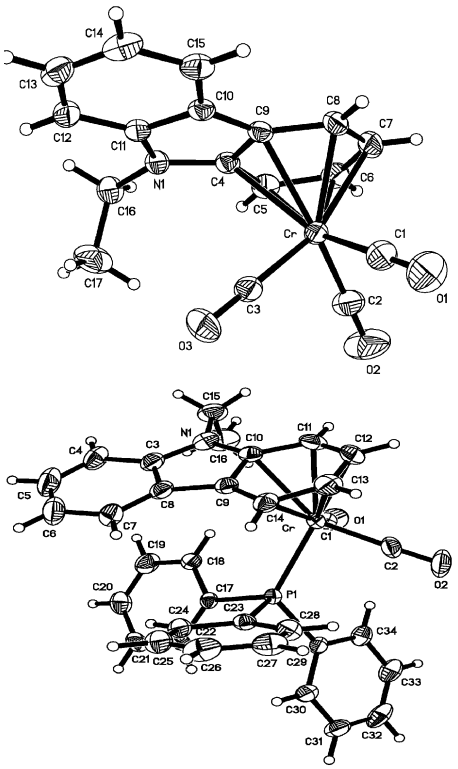

Fig. 2 ORTEP drawings of **2** (top) and **4** (bottom) with thermal ellipsoids at the 30% probability level.

Table 2 Selected bond lengths (Å) and angles (°) for **2** and **4**

2			
N(1)–C(4)	1.373(2)	N(1)–C(11)	1.392(2)
N(1)–C(16)	1.456(2)	C(4)–C(5)	1.392(3)
C(4)–C(9)	1.432(2)	C(8)–C(9)	1.406(3)
C(11)–C(12)	1.392(3)	C(10)–C(11)	1.400(2)
C(10)–C(15)	1.396(3)	Cr–C(1)	1.839(2)
Cr–C(2)	1.828(2)	Cr–C(3)	1.826(2)
C(1)–O(1)	1.142(3)	C(2)–O(2)	1.149(3)
C(3)–O(3)	1.149(2)		
C(4)–N(1)–C(11)	108.70(14)	C(5)–C(4)–C(9)	121.39(17)
C(8)–C(9)–C(4)	119.28(17)	C(15)–C(10)–C(11)	119.58(18)
C(14)–C(15)–C(10)	118.4(2)	N(1)–C(16)–C(17)	112.80(18)
4			
N(1)–C(3)	1.387(5)	N(1)–C(10)	1.379(5)
N(1)–C(15)	1.454(5)	C(10)–C(11)	1.411(6)
C(9)–C(10)	1.419(5)	C(9)–C(14)	1.403(5)
C(3)–C(4)	1.415(6)	C(3)–C(8)	1.404(6)
C(7)–C(8)	1.394(6)	Cr–C(1)	1.820(4)
Cr–C(2)	1.806(4)	Cr–P(1)	2.3209(9)
C(1)–O(1)	1.176(5)	C(2)–O(2)	1.170(5)
C(17)–P(1)–Cr	116.38(11)	C(23)–P(1)–Cr	112.33(11)
C(29)–P(1)–Cr	119.63(11)	C(18)–C(17)–C(22)	118.3(3)
C(28)–C(23)–C(24)	118.5(3)	C(34)–C(29)–C(30)	118.1(3)

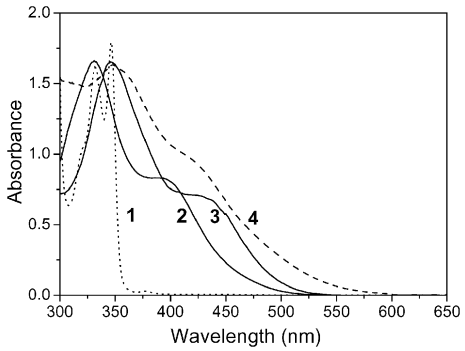

Fig. 3 Electronic absorption spectra of **1–4** in CH_2Cl_2 at 298 K.

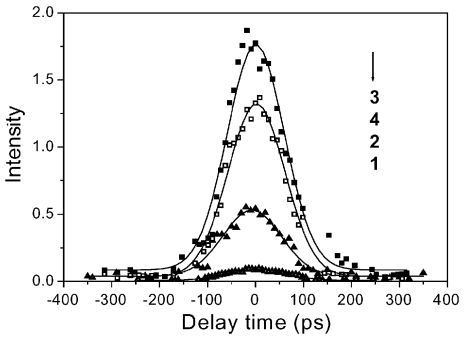

Fig. 4 Temporal DFWM signals of **1–4** in solution at 532 nm.

Linear optical properties

The electronic absorption spectra of molecules **1–4** were recorded in a variety of solvents with different polarities (*i.e.* cyclohexane, CH_2Cl_2 and DMF). Fig. 3 displays the spectra in CH_2Cl_2. Complexes **2–4** show two characteristic absorption bands in the 300–525 nm region.[3a–c,4,12] The absorption band at lower energy is assigned to MLCT arising from a charge transition from the chromium center to the π- and σ-bound ligands. The next band, at higher energy, is the most intense absorption, and arises from intraligand (IL) transitions with high oscillator strengths, mostly from π–π* transitions. The change from **2** to **3** causes a subtle red-shift, both in the lower energy band by 37 nm and in the higher energy band by 15 nm, indicating that a significant electron density transfer takes place from one metal center to the other through the carbazole conjugated system. This inference is also supported by the assumption that the chromium–carbonyl–arene fragment behaves electron-amphoterically to achieve charge redistribution within the dichromium system. Replacing a CO group in **2** with a phosphine ligand, as in **4**, is also found to lower the transition energy and to enhance the MLCT intensity, with a long tail extending far into the visible. We attribute the red-shifts to an increased delocalization of π-electrons into the carbazole unit by virtue of the metal-to-ligand π back-bonding interaction, because the PPh_3 ligand is electron-donating in nature and renders the chromium center more electron-rich. As can be seen from Table 3, the absorption bands of **2–4** are governed by a negative solvatochromism, which is typically more pronounced for the low energy absorption, indicating that the electronic ground state is more polar than the first excited state, and therefore an increase in solvent polarity causes a hypsochromic shift. This is also in accordance with the highly polar nature of these complexes, which can be attributed to dominant μ_z-dipole vector component directed from the carbazole plane to the metal center. To our surprise, in the case of **4**, the solvatochromic behavior in various solvent environments appears to be comparatively less significant. Clearly, such spectroscopic behavior is not a simple attribute of the electronic coupling between the carbazole unit and the metal atom, but is also associated with the nature of the other ligand. The charge-transfer from metal-to-ligand will give rise to a significant electronic asymmetry in the ground state, despite the lack of a good coincidence between the charge-transfer and dipole moment directions.[2d,4] The delocalization of π-electrons, on the other hand, will always increase the electronic symmetry and reduce the dipole difference between the ground and the excited states. This can help to explain the above result, where the red-shifts in the positions of the corresponding absorption peaks and reduced negative solvatochromism concur when a CO group is replaced by a PPh_3 ligand, as in **4**. Overall, a correct elaboration of the coordination environment and its solvatochromism will allow the tuning of the position of the absorption band to a desired wavelength, so as to create an optimal balance between near resonance and low α, as required in NLO devices.

Non-linear optical properties

Insert results from DFWM are given in Fig. 4, in which the solid line is the theoretical fitted curve with a Gaussian function. It is generally believed that the presence of any population grating induced by one-photon or two-photon absorption will result in an asymmetrically-temporal DFWM signal.[19] For each studied molecule, even with complex **4**, which has weak absorption at the measured wavelength of 532 nm, the measured signal did not show appreciable asymmetry either. This implies that the one-photon or two-photon contribution to the DFWM process is negligible. The third-order susceptibility, $\chi^{(3)}$, the non-linear refractive index, n_2, and the second-order hyperpolarizability, γ, were obtained, as listed in Table 3. The results reflect the fact that there is a significant

Table 3 MLCT band maxima and third-order non-linear optical coefficients for **1–4** in CH_2Cl_2, unless otherwise stated[a]

Compound	λ_{max}/nm (υ_{max}/cm^{-1})	$\chi^{(3)}/10^{-13}$ esu	$\gamma/10^{-30}$ esu	$n_2/10^{-11}$ esu	Comments
1		0.51	0.26	0.14	Off-resonance
2	409 (24450)[b]; 395 (25316); 387 (25840)[c]	6.41	2.54	1.70	Off-resonance
3	434 (23041)[b]; 432 (23148); 417 (23981)[c]	9.49	3.81	2.51	Off-resonance
4	424 (23585)[b]; 422 (23697); 416 (24038)[c]	8.24	3.27	2.18	Near-resonance

[a] γ and $\chi^{(3)}$ values were normalized to a concentration of 1.0×10^{-4} mol L^{-1}. [b] Measured in cyclohexane. [c] Measured in DMF.

contribution to the magnitude of the third-order non-linear response from chromium complexation, and that the measured $\chi^{(3)}$ and γ values are highly dependent on both the nature of the ligand and the extent of chromium tricarbonyl coordination by the carbazole ring. Cheng *et al.* reported that the γ values for several CBC complexes, measured by the third harmonic generation (THG) technique, are 2–21 $\times$ 10^{-36} esu.[5] The γ value of **2** is five or six orders of magnitude higher than that of the CBCs, confirming the potential advantage of the well-conjugated, planar and rigid ring of carbazole for enhancing the third-order response. Recently, Qian *et al.* investigated the third-order optical non-linearity of six 3,6-di-acceptor-substituent carbazole multi-polar chromophores using the single-beam Z-scan technique.[11a] The γ value of these organic molecules was estimated to be 1.5–2.9 $\times$ 10^{-33} esu, three orders of magnitude smaller than that of **2**, revealing the vital role of metal complexation. Although the γ values measured by the different techniques do not, in general, produce a quantitatively reliable comparison, since the experimental conditions and techniques used in each laboratory vary significantly, a qualitative trend for a systematically varied structure can still be deduced. A very large γ value up to 3.8 $\times$ 10^{-30} esu was obtained for complex **3**, in which two metal centers are simultaneously coordinated to the carbazole ring. In this case, the $Cr(CO)_3$ fragment functions as either a ground state acceptor or an excited state donor.[3a,4] These factors influence the nature of the charge-transfer processes between the metal and the carbazole ligand, or even inside the carbazole itself, producing a reciprocal push–pull organometallic architecture with carbazole-mediated metal–metal electronic interactions. The γ value of **4** appears to be larger than that of **2**, suggesting that the effect of ligand exchange on the organometallic moiety has a more subtle impact on non-linearity. The strong electron-donating ability of the PPh_3 group can permit more metal electrons in **4** to be involved in charge-transfer excitation than in **2**. The enhanced γ value of the former is considered to originate from an additional contribution of the MLCT excitation. **4** exhibits a strong charge-transfer absorption band, occurring in a relatively longer wavelength region, even though this band displays a small negative solvatochromism. Apart from the concern about making a judicious choice of ligands and metals to obtain the highest γ values, we are also interested in structural features of the carbazole ring and their ease of substitution by polymerizable groups. For this reason, these complexes can form polymers or be incorporated in polymers, either as pendant chains or into the polymer backbone, affording the possibility of introducing more polarizable groups into polymer chains than may be accessible in a solely organic system. Furthermore, the very bulky organometallic moiety may be helpful in reducing chromophore–chromophore electrostatic interactions, and in optimizing the chromophore loading level and the order parameter for the polymer matrix.[20]

Conclusions

In summary, we have synthesized three novel η^6-complexes of *N*-ethylcarbazole with $Cr(CO)_3$ and $Cr(CO)_2PPh_3$ moieties, and investigated their linear spectroscopic properties and third-order optical non-linearities. Chromium complexation can be one of the most effective tools for modulating and improving the non-linear response. It has been observed that the $\chi^{(3)}$ and γ values of these complexes are highly dependent on both the nature of the ligand and the extent of chromium tricarbonyl coordination by the carbazole ring. The corresponding non-linearity undergoes a strong enhancement when two metal centers are simultaneously coordinated to one carbazole molecule. A carbazole-mediated metal–metal electronic interaction is proposed to be associated with the amphoteric behavior of the $Cr(CO)_3$ fragment. Ligand exchange on the organometallic moiety also exerts a more subtle impact on the electronic structure of the molecule. The electron-donating ability of the PPh_3 ligand renders the carbazole ring more electron-rich, leading to a substantial improvement in the NLO response. These results suggest that the studied complexes are a particular class of compounds offering a promising route for third-order NLO studies. To gain more insight into the factors that affect the non-linear optical properties, we are continuing our studies on the rational modification of the organic structure, such as introducing functional groups onto the coordinated carbazole, in particular, by extending the carbazole conjugated system to macromolecular level.

Acknowledgements

We are grateful to the National Natural Science Foundation of China (grant no. 20274011) for generous financial support. We thank Dr Jie Sun for assistance in the X-ray data collection and refinement of complexes **2** and **4**.

References

1 (*a*) I. R. Whittall, A. M. McDonagh and M. G. Humphrey, *Adv. Organomet. Chem.*, 1999, **43**, 349; (*b*) U. Behrens, H. Brussaard, U. Hagenau, J. Heck, E. Hendrickx, J. Körnich, J. G. M. van der Linden, A. Persoons, A. L. Spek, N. Veldman, B. Voss and H. Wong, *Chem.–Eur. J.*, 1996, **2**, 98; (*c*) G. Rojo, F. Agulló-López, J. A. Campo, J. V. Heras and M. Cano, *J. Phys. Chem. B*, 1999, **103**, 11020; (*d*) M. P. Cifuentes, J. Driver, M. G. Humphrey, I. Asselberghs, A. Persoons, M. Samoc and B. Luther-Davies, *J. Organomet. Chem.*, 2000, **607**, 72; (*e*) W. F. Sun, C. C. Byeon, C. M. Lawson and D. Y. Wang, *Appl. Phys. Lett.*, 1999, **74**, 3254.

2 (*a*) J. Heck, S. Dabek, T. Meyer-Friedrichsen and H. Wong, *Coord. Chem. Rev.*, 1999, **190–192**, 1217; (*b*) G. de la Torre, P. Vázquez, F. Agulló-López and T. Torres, *Chem. Rev.*, 2004, **104**, 3723; (*c*) H. S. Nalwa, *Appl. Organomet. Chem.*, 1991, **5**, 349; (*d*) D. R. Kanis, M. A. Ratner and T. J. Marks, *J. Am. Chem. Soc.*, 1992, **114**, 10338.

3 (*a*) T. M. Gilbert, F. J. Hadley, C. B. Bauer and R. D. Rogers, *Organometallics*, 1994, **13**, 2024; (*b*) T. J. J. Müller, M. Ansorge and H. J. Lindner, *Chem. Ber.*, 1996, **129**, 1433; (*c*) T. J. J. Müller and J. Blümel, *J. Organomet. Chem.*, 2003, **683**, 354; (*d*) C. A. Merlic, B. N. Hietbrink and K. N. Houk, *J. Organomet. Chem.*, 2001, **66**, 6738; (*e*) C. A. Merlic, J. C. Walsh, D. J. Tantillo and K. N. Houk, *J. Am. Chem. Soc.*, 1999, **121**, 3596.

4 T. J. J. Müller, A. Netz, M. Ansorge, E. Schmälzlin, C. Bräuchle and K. Meerholz, *Organometallics*, 1999, **18**, 5066.

5 L. T. Cheng, W. Tam, G. R. Meredith and S. R. Marder, *Mol. Cryst. Liq. Cryst.*, 1990, **189**, 137.

6 G. H. Wang, C. W. Yuan, H. W. Wu and Y. Wei, *J. Appl. Phys.*, 1995, **78**, 2679.

7 (*a*) V. S. Mylnikov, *Adv. Polym. Sci.*, 1994, **115**, 1–88; (*b*) J. M. Pearson and M. Stolka, *Poly(N-vinylcarbazole)*, Gordon and Breach, New York, 1981.

8 (*a*) B. Kippelen, K. Tamura, N. Peyghambarian, A. B. Padias and H. K. Hall, *Phys. Rev. B: Condens. Matter*, 1993, **48**, 10710; (*b*) Z.-H. Peng, Z.-N. Bao and L.-P. Yu, *J. Am. Chem. Soc.*, 1994, **116**, 6003.
9 (*a*) W. E. Moerner and S. M. Silence, *Chem. Rev.*, 1994, **94**, 127; (*b*) G. G. Mallioras, V. V. Krasnikov, H. J. Balink and G. Hadziaonnou, *Appl. Phys. Lett.*, 1994, **65**, 262.
10 M. Nisoli, V. Pruneri, V. Magni, S. De Silverstri, G. Dellenpiane, D. Comoretto, C. Cuniberti and J. Le Moigne, *Appl. Phys. Lett.*, 1994, **65**, 590.
11 (*a*) Q. Ying, B.-P. Lin, Y.-M. Sun, G. Wang, Y.-P. Cui and C.-W. Yuan, *Acta Chim. Sin.*, 2005, **63**, 2141; (*b*) X.-W. Zhan, Y.-Q. Liu, D.-B. Zhu, X.-C. Liu, G. Xu and P.-X. Ye, *Chem. Phys. Lett.*, 2001, **343**, 493; (*c*) X.-W. Zhan, Y.-Q. Liu, D.-B. Zhu, X.-C. Liu, G. Xu and P.-X. Ye, *Chem. Phys. Lett.*, 2002, **362**, 165.
12 K.-Y. Shen, X.-H. Tian, J.-H. Zhong, J.-P. Lin, Y. Shen and P.-Y. Wu, *Organometallics*, 2005, **24**, 127.
13 J. V. Grazulevicius, P. Strohriegl, J. Pielichowski and K. Pielichowski, *Prog. Polym. Sci.*, 2003, **28**, 1297.
14 (*a*) G. M. Sheldrick, *SHELXS-97, Program for solution of crystal structures*, University of Göttingen, Germany, 1997; (*b*) G. M. Sheldrick, *SHELXL-97, Program for refinement of crystal structures*, University of Göttingen, Germany, 1997.
15 D. V. G. L. N. Rao, F. J. Aranda, J. F. Roach and D. E. Remy, *Appl. Phys. Lett.*, 1991, **58**, 1241.
16 K. Kandasamy, S. J. Shetty, P. N. Puntambekar, T. S. Srivastava, T. Kundu and B. P. Singh, *Chem. Commun.*, 1997, **13**, 1159.
17 (*a*) K. H. Dötz, J. Stendel, Jr, S. Müller, M. Nieger, S. Ketrat and M. Dolg, *Organometallics*, 2005, **24**, 3219; (*b*) K. H. Dötz, N. Szesni, M. Nieger and K. Nättinen, *J. Organomet. Chem.*, 2003, **671**, 58; (*c*) E. P. Kündig, V. Desobry, C. Grivet, B. Rudolph and S. Spichiger, *Organometallics*, 1987, **6**, 1173; (*d*) E. P. Kündig, C. Perret and S. Spichiger, *J. Organomet. Chem.*, 1985, **286**, 183.
18 (*a*) S. C. Jones, T. Hascall, S. Barlow and D. O'Hare, *J. Am. Chem. Soc.*, 1998, **124**, 11610; (*b*) S. Barlow and D. O'Hare, *Chem. Rev.*, 1997, **97**, 637; (*c*) Y. Oprunenko, I. Gloriozov, K. Lyssenko, S. Malyugina, D. Mityuk, V. Mstislavsky, H. Günther, G. von Firks and M. Ebener, *J. Organomet. Chem.*, 2002, **656**, 27.
19 M. T. Zhao, M. Samoc, P. N. Prasad, B. A. Reinhardt, M. R. Unroe, M. Prazak, R. C. Evers, J. J. Kane, C. Jariwala and M. Sinsky, *Chem. Mater.*, 1990, **2**, 670.
20 P. Wang, P. W. Zhu, C. Ye, A. E. Asato and R. S. Liu, *J. Phys. Chem. A*, 1999, **103**, 7076.